Proceedings of the 2nd ITB Graduate School Conference

Strengthening Multidisciplinary Research to Enhance its Impact on Society
July 21, 2022

Computational Modelling of Steady State Linear Elasticity using Least Square Moving Particle Semi-Implicit Method

Dewangga Alfarisy* & Lavi Rizki Zuhal

Faculty of Mechanical and Aerospace Engineering, Bandung Institute of Technology *Email: dewangga.alfarisy@gmail.com

Abstract. Least Square Moving Particle Semi-Implicit (LSMPS) Method is a particle based spatial differential operator designed to solve various continuum mechanics problems by using particle-based method computation. LSMPS is able to solve the spatial derivative of a particle at any given locations when it has sufficient number of neighboring particles even if the neighboring particles is randomly distributed in contrast to standard finite difference method where the particle must be distributed in a typical cartesian grid. In this study, the LSMPS operator will be used to solve steady linear elasticity problems in both two-dimensional and three-dimensional domain. The result obtained from LSMPS numerical simulation is compared to the respective analytical solution, empirical solution, or available commercial software ANSYS. In this study, the simulation time required for each problem using the LSMPS discretization is also the research interest and is tabulated as a reference for the reader.

Keywords: linear elasticity; particle-based simulation; and structure analysis.

1 Introduction

Nowadays, the elasticity problems mostly are solved by applying the finite element method (FEM) on the elasticity governing equations. However, there are certain requirements in discretization by finite element method, such as the requirement to generate a proper mesh grid for the domain and the transformation of the governing equation into the weak-form or integral form in order to solve the elasticity governing equation by FEM. This Finite Element Method is very popular and many commercial software employs this method such as ANSYS®.

Particle based methods, unlike the mesh-based method counterpart has been long developed. In the last 20 years, there are many particle-based method developed for calculating spatial derivation as described by Chen et.al. in [1]. One of the popular particle-based method SPH (Solid Particle Hydrodynamics) are able to solve the elasticity differential equations without the usage of mesh and it is able to solve the governing equations directly in its strong form (differential form). This leads to a less complex discretization and solving procedure while also helps to support for large deformation simulation as the particle can move freely

ISSN: 2963-718X

compared to mesh-based method. Most of SPH methods implemented for elasticity problem however are designed to solve for dynamic elasticity problem such as Gray (2001) in [2]. However, the dynamic elasticity formulation is very inefficient to be used to solve for static elasticity problem due to the high computational effort required.

Therefore, a more efficient solution which solves specifically for the static elasticity problem is needed. One of the methods that has been used for solving the static elasticity problem is DC-PSE (Discretization Corrected Particle Strength Exchange) method developed by Bourantas (2018) in [3] has successfully applies this particle-based discretization method in hybrid with the standard finite difference method to solve for the static linear elasticity problems.

Another promising particle-based discretization method is the Least Square Moving Particle Semi-Implicit (LSMPS) Method introduced by Tamai & Koshizuka (2014) in [4] which are the further development using least square model of the older moving particle semi-implicit (MPS) method developed by Koshizuka & Oka (1996) in [5] that has been booked by Koshizuka et.al. (2018) in [6]. This method is mainly used for calculating particle-based spatial derivative for application in fluid dynamics, and nuclear dynamics.

Considering the other particle-based discretization method that discussed before, the author has decided to use a full LSMPS discretization method for the whole domain of the elastic solid. The author intends to measure the accuracy of full LSMPS discretization method and its computational time for solving the static elasticity problems.

2 Theoretical Basis

2.1 Elasticity

Deformation of a solid material is caused by the application of load. While elasticity is the ability of a material to resist this deformation. A material is determined as an elastic material when its shape returns to its original shape when the applied load is removed. The measurement for elasticity is defined by elastic modulus such as the Young's modulus which connects the factor of stress and strain of the material due to compression or tension loading. The Young's modulus relation with stress and strain linearly calculated as in Eq. 1 as described by Bauchau & Craig (2009) in [7].

$$\sigma = E.\varepsilon \tag{1}$$

Solid materials such as aluminum and steel undergoes this elastic deformation when deformation is sufficiently small and the material's stress does not exceed its yield stress value. When the deformation exceeds its elastic limit, plastic deformation occurs on the material and the stress-strain relationship cannot be approximated to be linear. This stress strain relation is shown using the general stress-strain curve for typical isotropic material in Figure 1 as described in Sadd (2021) in [8].

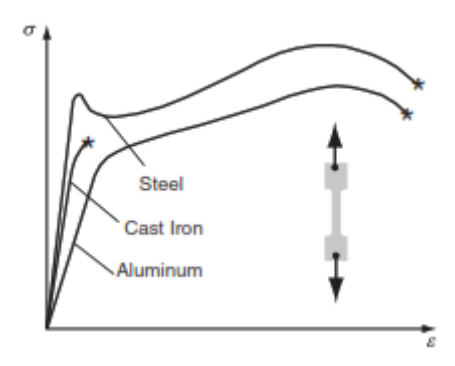


Figure 1 General stress-strain curve in elasticity for selected materials.

2.2 Linear Elasticity

The linearization assumption of an elasticity model is only valid to be used for very small strain or deformations where the material does not exceed its yielding limit value (Yield Stress). Without using the linear assumption, the strain of a material is related to its displacement by Eq. 2 and 3 for lagrangian and eulerian space respectively as described by Sadd (2019) in [9].

$$\mathbf{\varepsilon} = \frac{1}{2} \left[\nabla \mathbf{u} + (\nabla \mathbf{u})^T - (\nabla \mathbf{u})^T \cdot \nabla \mathbf{u} \right]$$
 (2)

$$\mathbf{\Sigma} = \frac{1}{2} [\nabla_{\mathbf{x}} \mathbf{u} + (\nabla_{\mathbf{x}} \mathbf{u})^{T} - (\nabla_{\mathbf{x}} \mathbf{u})^{T} \cdot \nabla_{\mathbf{x}} \mathbf{u}]$$
(3)

Using the linearization assumption, the relation can be simplified into the Eq. 4 as described by Sadd (2021) in [8].

$$\boldsymbol{\varepsilon} \cong \boldsymbol{\Sigma} = \frac{1}{2} [\nabla \boldsymbol{u} + (\nabla \boldsymbol{u})^T] \tag{4}$$

The constitutive equation is needed for the stress-strain relationship. The constitutive equation used is the Hooke's law for linear isotropic elastic material which is shown as Eq. 5 by Bower (2010) in [10].

$$\sigma = \lambda . tr(\varepsilon) . I + 2\mu \varepsilon \tag{5}$$

Where λ and μ are the Lamé constants and shear modulus respectively defined by Bower (2010) in [10] as Eq. 6 and Eq. 7 respectively.

$$\lambda = \frac{v.E}{(1+v)(1-2v)} \tag{6}$$

$$\mu = \frac{E}{2.(1+\nu)} \tag{7}$$

These linear elasticity relations will be used to solve the Navier-Cauchy linear elasticity equations in terms of displacement.

2.3 Linear Elasticity Governing Equation

The general momentum equilibrium differential equations for elasticity problem consists of inertial forces, body forces, and the stresses acting on the material. This is shown in in the following equation as in Bower (2010) in [10].

$$\rho \frac{\partial V}{\partial t} = \nabla \cdot \mathbf{\sigma} + \mathbf{f} \tag{9}$$

Using the linearization assumption, the relation can be simplified into the Eq. 10.

$$\nabla \cdot \mathbf{\sigma} = -\mathbf{f} \tag{10}$$

For the boundary conditions, the known property can either be the stresses applied on the surface (Neumann boundary conditions) or the displacement of the particles (Dirichlet boundary conditions). For the Neumann boundary condition, the equation is stated in Eq. 11.

$$\mathbf{u} = \mathbf{d} \tag{11}$$

For the Dirichlet boundary condition, the boundary equation is stated in Eq. 12.

$$\sigma. n = t \tag{12}$$

2.4 Least-Square Moving Particle Semi-Implicit Method

Least Squares Moving Particle Semi-implicit (LSMPS) Method was developed by Tamai and Koshizuka (2014) [4] to simulate flow in incompressible flow with free surfaces. This method is the improvement from the Moving Particle Semi-implicit (MPS) Method which was also developed by Koshizuka and has been written in a book by Koshizuka (2018) in [6]. The improvement of LSMPS method from MPS which had been made is minimizing the error using weighted least squares function. In this simulation the idea of LSMPS is adopted to calculate the spatial derivatives.

The main equation for LSMPS spatial approximation convolution as in Eq. 9.

$$\mathbf{D}_{x}f^{h}(\mathbf{x}_{i}) = \mathbf{H}_{r_{s}}\mathbf{M}_{i}^{-1}\mathbf{b}_{i} \tag{9}$$

The H_{r_s} matrix is the monomial basis for the LSMPS method as in Eq. 10.

$$H_{r_s} := diag\left(\left(r_s^{-|a|}a!\right)_{1 \le |a| \le p}\right) \tag{10}$$

The M_i and b_i matrix is the least square approximation measure as in Eq. 11 and 12 respectively.

$$\mathbf{M}_{i} \coloneqq \sum_{j \in \Lambda_{i}} \left(\mathbf{\omega} \left(\left| \left| \mathbf{x}_{j} - \mathbf{x}_{i} \right| \right| \right) \mathbf{p} \left(\frac{\mathbf{x}_{j} - \mathbf{x}_{l}}{r_{s}} \right) \mathbf{p}^{T} \left(\frac{\mathbf{x}_{j} - \mathbf{x}_{l}}{r_{s}} \right) \right)$$
(11)

$$\boldsymbol{b_i} \coloneqq \sum_{j \in \Lambda_i} \left(\boldsymbol{\omega} \left(\left| \left| \boldsymbol{x_j} - \boldsymbol{x_i} \right| \right| \right) \boldsymbol{p} \left(\frac{\boldsymbol{x_j} - \boldsymbol{x_i}}{r_s} \right) \left(\boldsymbol{f}(\boldsymbol{x_j}) - \boldsymbol{f}(\boldsymbol{x_i}) \right) \right)$$
(12)

The ω is the weighting function used in the formulation, the weighting function used is as stated in Eq. 13.

$$\boldsymbol{\omega}(\boldsymbol{x}, r_e) = \begin{cases} \left(1 - \frac{||\boldsymbol{x}||}{r_e}\right)^2 & , 0 \le ||\boldsymbol{x}|| < r_e \\ 0 & , ||\boldsymbol{x}|| \ge r_e \end{cases}$$
 (13)

3 Computational Modelling

3.1 Program Structure

The code developed for this project is written in Python to obtain simple and efficient code by benefiting from the reliable and simple vectorization syntax in Python. For the linear algebra library, the scipy library is utilized, in order to calculate the sparse matrix manipulation feature. The plotting then will use matplotlib library.

3.2 Test Case Problem

The test case problems are simulated using the code to be compared with analytical or commercial software available. The test cases consists of both 2D and 3D cases with variation in problem sizes and geometry.

3.2.1 2D Cantilever Beam with Distributed Load

The first test case is a simple 2D cantilever beam that given distributed loading on its top. The boundary used for this simulation is a no displacement boundary (Dirichlet boundary) on the left side of the beam to simulate the cantilever effect, with traction boundary (Dirichlet boundary) on the top side of the beam with traction value W, and traction-free boundaries (Neumann boundary) on bottom and right side of the beam. For this test case, the numerical deflection in y-axis is compared with its respective analytical solution using Euler's beam deflection equation by Hibbeler (2003) in [11]. The schematics for this test case and its details is given in Figure 2 and Table 1.

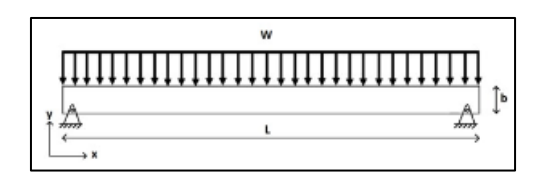


Figure 2 Test Case 1: 2D cantilever beam with distributed load.

Table 1 Mechanical Properties of Test Case 1.

Parameter	Value	Unit
Young's Modulus (E)	200	GPa
Poisson's Ratio (v)	0.3	
L	1	m
b	0.05	m
Thickness	0.001	m
$\mathbf{W}_{ ext{max}}$	20000	kN/m^2

The analytical solution provided by Hibbeler (2003) in [11] is stated in Eq. 13.

$$w(x) = \frac{-Wx^2}{24EL}(x^2 - 4Lx + 6L^2)$$
 (13)

3.2.2 2D Hollowed Plate with Tensile Load

The second test case is the stress concentration of a single hollowed plate given tension load on its longitudinal axis. The boundaries used for this simulation is a no displacement boundary on the left side of the plate, traction boundary on the right side of the beam, and traction free boundaries on the top, bottom, and the hole of the plate. For this test case, the stress concentration from the LSMPS numerical calculation is compared to the results from empirical formula by Pilkey (2005) in [12]. and commercial finite element software (ANSYS®). The maximum stress concentration of the plate is expected to occur directly above

and below the circular hole. The schematics for this test case and its details is given in Figure 3 and Table 2.

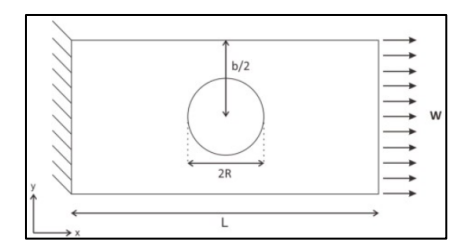


Figure 3 Test Case 2: 2D hollowed plate with tensile load.

 Table 2
 Mechanical Properties of Test Case 2.

Parameter	Value	Unit
Young's Modulus (E)	200	GPa
Poisson's Ratio (ν)	0.3	
L	0.6	m
b	0.3	m
Thickness	0.001	m
$\mathbf{W}_{ ext{max}}$	10000	kN/m^2

The analytical solution provided by Pilkey (2005) in [12] is stated in Eq. 14 and Eq. 15.

$$K_t = 3 - 3.14 \left(\frac{2R}{h}\right) + 3.667 \left(\frac{2R}{h}\right)^2 - 1.527 \left(\frac{2R}{h}\right)^3$$
 (14)

$$\sigma_{max} = K_t \frac{1}{1 - \left(\frac{2R}{h}\right)} \tag{15}$$

3.2.3 3D Cantilever Beam with Shear Load

The third test case is a simple 3D cantilever beam that given shear loading on its side. The boundary used for this simulation is a no displacement boundary (Dirichlet boundary) on the left side of the beam to simulate the cantilever effect, with traction boundary (Dirichlet boundary) on the right side of the beam with traction value W, and traction-free boundaries (Neumann boundary) on top and bottom side of the beam. For this test case, the numerical deflection in z-axis is compared with its respective analytical solution using Euler's beam deflection equation by Hibbeler (2003) in [11]. The schematics for this test case and its details is given in Figure 4 and Table 3.

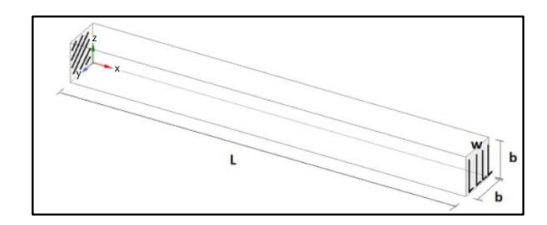


Figure 4 Test Case 3: 3D cantilever beam with shear load.

Table 3 Mechanical Properties of Test Case 3.

Parameter	Value	Unit
Young's Modulus (E)	200	GPa
Poisson's Ratio (ν)	0.3	
L	1	m
b	0.05	m
W	10000	kN/m^2

The analytical solution provided by Hibbeler (2003) in [11] is stated in Eq. 16.

$$w(x) = \frac{-Wx^2}{6EL}(3L - x) \tag{16}$$

3.3 Difference Calculation

In this research, the difference will be calculated using two different method, maximum relative difference, and RMSE (root means square error). The calculation for each difference calculation will be tabulated in Eq. 17 and Eq. 18 respectively.

Relative Difference =
$$\left| \frac{y_{LSMPS} - y_{Euler}}{y_{Euler}} \right|_{\delta = \delta_{max}}$$
(17)
$$RMSE = \sqrt{\frac{\sum_{i=1}^{n} (y_{LSMPS} - y_{Euler})^{2}}{n}}$$
(18)

4 Results and Analysis

The numerical simulation for this research is done using a Python compiler from Jupyter Notebook on ASUS® ROG GL553VD Laptop with Windows 10 OS and equipped with 8 cores Intel® CORETM i7 7700HQ processor and 12 Gb of RAM. Therefore, most of the computational time in this project is measured from start to finish by using the respective laptop specification. The result from LSMPS method then will be compared with the respective analytical, empirical, or commercial software ANSYS.

4.1 2D Cantilever Beam with Distributed Load

For the beam geometry, the particle distribution is using cartesian grid with constant particle spacing h. This particle distribution is illustrated in Figure 5 with constant particle spacing of 0.00143 m with 24500 particles.

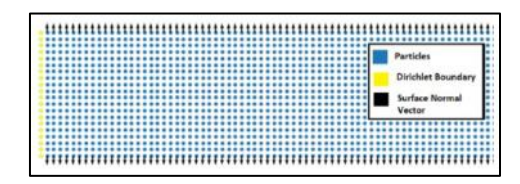


Figure 5 Particle distribution of test case 1.

The simulation using LSMPS for this case is requiring a computational time of 235 seconds to simulate the model with 24500 particles with a relative difference of 0.28 % and RMSE of 2.18E-6. The detailed report of the result is tabulated in Table 4.

 Table 4
 Summary of Test Case 1 Results

Parameters	Value	Unit	
Number of particles	24500		
LSMPS maximum y-displacement	-0.001203	m	
Analytical maximum y-displacement	-0.0012	m	
Relative difference	0.28	%	
RMSE	2.18E-6		

The von mises stress, y-displacement, and deflection comparison then can be tabulated in Figure 6, 7, and 8 respectively.

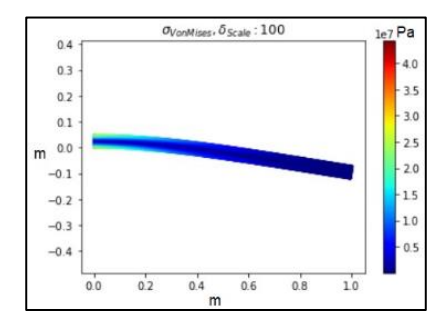


Figure 6 Von mises contour of LSMPS method on test case 1

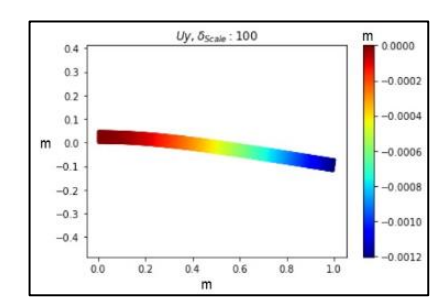


Figure 7 Y-displacement contour of LSMPS method on test case 1.

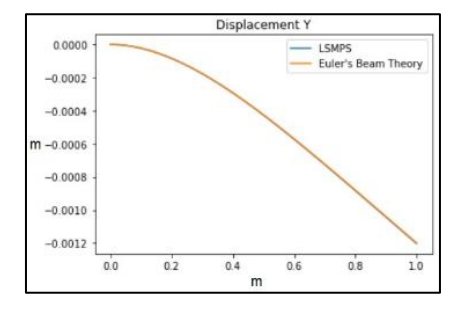


Figure 8 Y-Deflection comparison between LSMPS method and analytical.

4.2 2D Hollowed Plate with Tensile Load

For the plate geometry, the particle distribution is using cartesian grid with constant particle spacing h. This particle distribution is using constant particle spacing of 0.00133 m with 91754 particles as described in Figure 9.

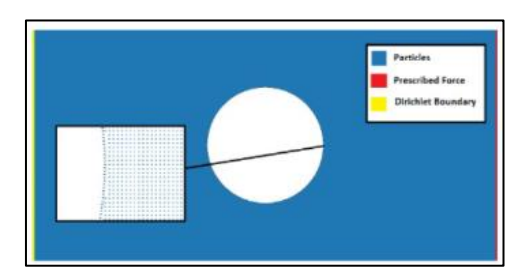


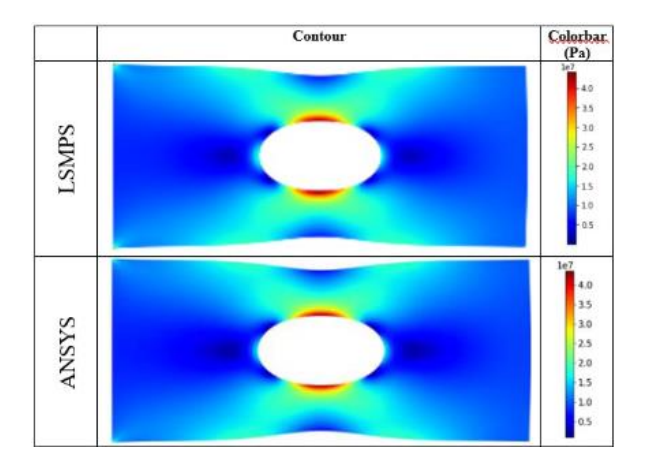
Figure 9 Particle distribution of test case 2.

The simulation using LSMPS for this case is requiring a computational time of 1220 seconds to simulate the model with 24500 particles with a relative difference of 2.31 %. The detailed report of the result is tabulated in Table 5.

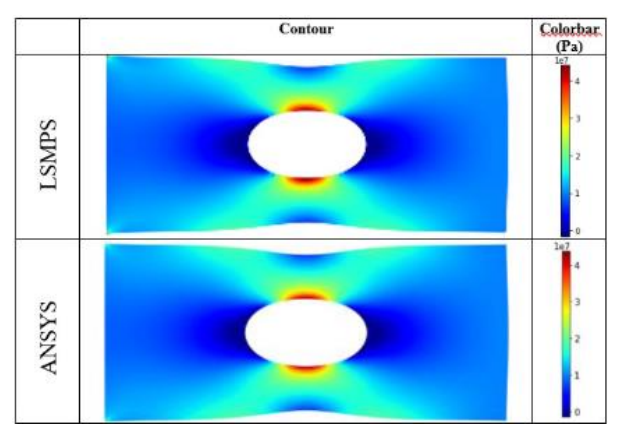
Parameters Value Unit 2.1559 kN/m^2 LSMPS maximum x-dir. stress kN/m^2 44114 $kN\!/m^2$ Empirical maximum x-dir. stress 43188 ANSYS maximum x-dir. stress 43731 Relative difference LSMPS to analytical 2.31 % Relative difference LSMPS to ANSYS 0.87 %

Table 5 Summary of test case 2 results

The von mises stress, and x-direction stress comparison then can be tabulated in Figure 10, and 11 respectively.



 $\label{eq:Figure 10} \textbf{Figure 10} \ \text{Von mises stress contour of LSMPS and ANSYS comparison on test } \\ \text{case 1}$



 $\begin{tabular}{ll} \textbf{Figure 11} X-direction stress contour of LSMPS and ANSYS comparison on test case 1 \\ \end{tabular}$

4.3 3D Cantilever Beam with Shear Load

For the beam geometry, the particle distribution is using cartesian grid with constant particle spacing h. This particle distribution is using constant particle spacing of 0.005 m with 80000 particles.

The simulation using LSMPS for this case is requiring a computational time of 11794 seconds to simulate the model with 24500 particles with a relative difference of 2.04 % and RMSE of 1.99E-5 to the analytical result. Compared to the commercial FEM software ANSYS, the relative difference is 2.04%. The detailed report of the result is tabulated in Table 6.

Parameters	Value	Unit
LSMPS maximum z-displacement	-0.00199	m
Analytical maximum z-displacement	-0.00204	m
ANSYS maximum z-displacement	-0.00204	m
LSMPS relative difference to analytical	2.04	%
LSMPS relative difference to ANSYS	2.04	%
LSMPS RMSE to analytical	1.99E-5	

 Table 6
 Summary of test case 3 results

The von mises stress, y-displacement, and deflection comparison then can be tabulated in Figure 12, 13, and 14 respectively.

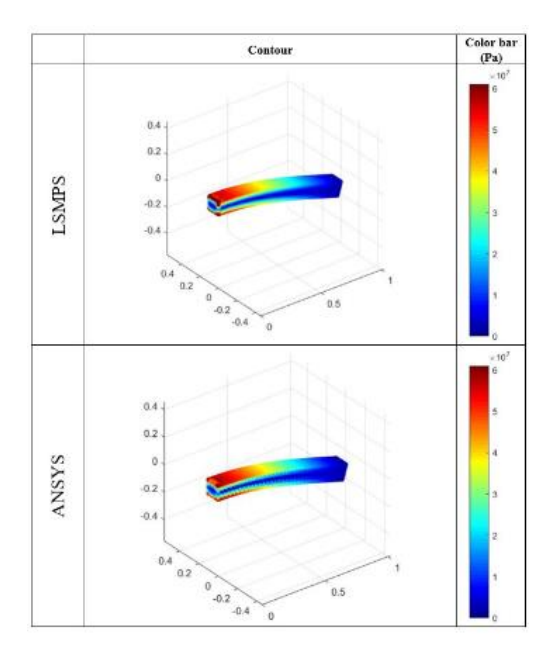


Figure 12 Von mises contour of LSMPS method on test case 3.

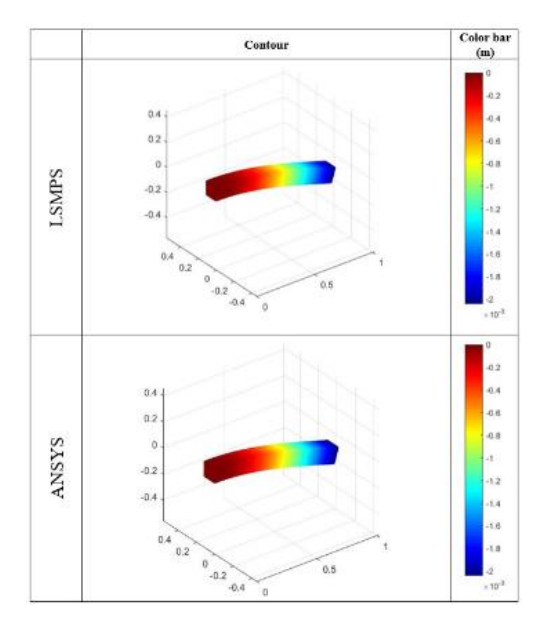


Figure 13 Z-displacement contour of LSMPS method on test case 3.

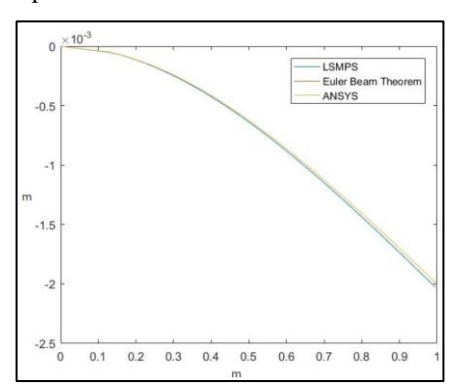


Figure 14 Z-deflection comparison between LSMPS method and analytical.

4.4 Summary

Based on the result of LSMPS method on solving both 2D and 3D cases, the results can be summarized in Table 7.

Case	2D/3D	Particle Number	Relative Difference (%)	RMSE
1	2D	24500	0.28	2.18E-6
2	2D	91754	2.31	-
3	3D	64000	2.04	1.99E-5

 Table 7
 Mechanical Properties of Test Case 1.

5 Conclusion

Based on the LSMPS simulation result using the developed code, it can be concluded that the LSMPS differential operator is able to achieve high accuracy for steady-state linear elasticity problem. The static elasticity approximation result developed using LSMPS is yielding at most 2.31% difference with commercial software, analytical, or empirical result.

Acknowledgement

We would like to thank Lab Flow Science and Engineering of Faculty of Mechanical and Aerospace Engineering, Bandung Institute of Technology for endless support and the continuous research program.

Nomenclature

 \boldsymbol{E} : Young's modulus λ : Lamé constants

 ε : Strain in langrangian coordinate μ : Shear modulus

 \boldsymbol{u} : Deformation w(x): Analytical deflection

 Σ : Strain in eulerian coordinate I: Moment of inertia

 σ : Stress L: Beam length

f: Applied force x: x-coordinate position in beam

 H_{r_s} : Hrs matrix of LSMPS W: Applied force in analytical approximation

 M_i : Mi matrix of LSMPS K_t : Plate constant approximation

R: Radius

 ω : Weight function of LSMPS approximation ν : Poisson's ratio

References

[1] Chen, Jiun-Shyan, Hillman, Michael, Chi, & Sheng-Wei, Meshfree Methods: Progress Made after 20 Years. Journal of Engineering Mechanics, 143(4), 04017001–. doi:10.1061/(ASCE)EM.1943-7889.0001176, 2017.

- [2] Gray, J. P., Monaghan, J. J. & Swift, R. P., *SPH Elastic Dynamics*, Computer Methods in Applied Mechanics and Engineering, vol. 190, no. 49-50, pp. 6641-6662, 2001.
- [3] Bourantas G. C., Mountris K. A., & Loukopoulos V., Strong-form approach to elasticity: Hybrid finite difference-meshless collocation method (FDMCM), Applied Mathematical Modelling, vol. 57, pp. 316-338, 2018.
- [4] Tamai, T. & Koshizuka S. *Least Squares Moving Particle Semi-Implicit Method*, Computational Particle Mechanics vol. 1, pp. 277-305, 2014.
- [5] Koshizuka, S. and Oka, Y., *Moving Particle Semi-Implicit Method for Fragmentation of Incompressible Fluid*, Nuclear Science and Engineering, 123, pp. 421-434. 1996.
- [6] Koshizuka, S., Shibata, K., Kondo M., and Matsunaga, T., *Moving Particle Semi-Implicit Method*, Tokyo: Academic Press, 2018.
- [7] Bauchau, O.A. & Craig, J.I., Structural Analysis with Application to Aerospace Structures, Dordrecht: Springer. 2009.
- [8] Sadd, M.H. *Elasticity Theory, Applications, and Numerics Fourth Edition*, London: Academic Press, 2021.
- [9] Sadd, M.H., Continuum mechanics modeling of material behavior, London: Elsevier, 2019.
- [10] Bower, Allan F. *Applied Mechanics of Solids*, Boca Raton, FL: CRC Press, 2010.
- [11] Hibbeler, R. C., *Mechanics of Materials*, Upper Saddle River, NJ: Pearson Education, 2003.
- [12] Pilkey, W.D., Formulas for Stress, Strain, and Structural Matrices, Hoboken, NJ: John Wiley & Sons, 2005.